Surfactant Adsorption at the Salt/Water Interface: Comparing the Conformation and Interfacial Water Structure for Selected Surfactants

Kevin A. Becraft and Geraldine L. Richmond*

Department of Chemistry, University of Oregon, Eugene, Oregon 97403-1253

Received: September 8, 2004; In Final Form: January 4, 2005

We report in situ spectroscopic measurements monitoring the adsorption of a series of carboxylate surfactants onto the surface of the semisoluble, ionic solid fluorite (CaF_2). We employ the surface-specific technique, vibrational sum-frequency spectroscopy (VSFS), to examine the effect that surfactant adsorption has on the bonding interactions and orientation of interfacial water molecules through the alteration of the electric properties in the interfacial region. In addition, we report on the chain length and headgroup dependence of the formation of hydrophobic self-assembled monolayers on the surface of the solid phase. Differences in chain length and headgroup functionality lead to large changes in the adsorption behavior and structuring of the monolayers formed and the interactions of interfacial water molecules with these monolayers. Fundamental studies such as these are essential for understanding the mechanisms involved in the surfactant adsorption process, information that is important for industrially relevant processes such as mineral ore flotation, waste processing, and petroleum recovery.

Introduction

The adsorption of surfactant ions onto the surface of solid phases is an important method to alter and control the surface properties of these phases.[1−3] Modification of the surface charge, the surface hydrophobicity, and the structure of solvent molecules in the interfacial region are all important characteristics that can be altered to suit a particular need. In the mineral processing industry, the modification of the surface properties of different mineral phases plays a key role in their separation via the froth flotation process.[4] The formation of ordered surfactant structures with specific orientations designed to achieve selectivity in these systems is highly dependent on the properties of the solid phase, the surrounding aqueous phase solvent structure, and the surfactant ion composition. To optimize the separation of different solid phases, a detailed knowledge of the adsorption process and the behavior of different surfactant molecules is necessary.

Fluorite (CaF_2) is a sparingly soluble solid that is the most important source material in the production of hydrofluoric acid,[5] in the refining of lead and antimony, and in the production of clear, colorless lenses used for a variety of optical applications.[6] The separation of this solid phase from other calcium-containing and silicate minerals is typically carried out via the froth flotation process. Of particular importance to these separations are fatty acid collectors (surfactants) containing a carboxylate headgroup and a hydrocarbon chain of differing lengths and compositions. The adsorption of these ions onto hydrophilic CaF_2 solids creates hydrophobic interfaces that can attach to air bubbles generated during the froth flotation process, allowing for their separation from other mineral phases in solution. The efficiency of these separations are governed, in part, by the ability to form strongly hydrophobic surfaces on the solid phase. The adsorption density and structuring of the adsorbed surfactant molecules (and therefore the degree of hydrophobicity) are highly dependent on their chain length and composition. In addition, interfacial water molecule structure is also of considerable importance in the overall floatability of the solid phase.[7] Therefore, studies to elucidate the effects of different surfactant ion compositions on the overall adsorption behavior and interfacial water structure are necessary.

Complicating this endeavor is the relative lack of experimental techniques available to provide molecular-level information about the interfacial region, in situ, during the surfactant adsorption process. Experiments such as potentiometric titrations,[6] ζ potential measurements,[8] IR spectroscopy,[9,10] and bulk adsorption studies[11−14] are useful in studying bulk properties such as solubility and adsorption density but cannot give molecular-level information about the interfacial region. Other types of molecular-level experiments such as Fourier transform infrared internal reflection spectroscopy (FTIR-IRS)[15,16] and diffuse reflectance infrared Fourier transform (DRIFT)[17,18] spectroscopy can monitor directly or extrapolate molecular-level information but require extensive removal of signal from the vast number of molecules in the bulk, making interface-specific arguments difficult. In contrast, vibrational sum-frequency spectroscopy (VSFS) is an interface-specific technique that can give in situ, molecular-level information for a variety of interfacial species, thus avoiding these complications. It is well-suited to examine water structure and surfactant adsorption at the CaF_2/H_2O interface that previous studies in our group have demonstrated.[19−22]

In this paper, we report VSFS experiments monitoring the adsorption behavior of a series of long- and short-chain carboxylate surfactants on the surface of CaF_2. We have studied the adsorption behavior of the negatively charged, 18-carbon alkyl chain carboxylate ions stearate (straight *n*-alkyl chain) and oleate (C_9 cis double bond) and the shorter carboxylate ions decanoate (C_{10}) and hexanoate (C_6). We compare the adsorption behavior of these surfactants to our previously published studies[20,21] of dodecyl sulfate adsorption onto the CaF_2 surface. We examine the affect of surfactant adsorption on the bonding

* Author to whom correspondence should be addressed. Fax: 541-346-5859. E-mail: richmond@uoregon.edu.

10.1021/jp045938j CCC: $30.25
Published on Web 03/02/2005

characteristics and orientation of interfacial water molecules. Our results indicate that there are significant changes to the adsorption density, the structure of the adsorbed self-assembled monolayer, the charge in the interfacial region, and the overlying water molecule network as a function of the composition of the various adsorbed surfactant ions. Significant differences in the concentration and time dependence of the adsorption process are also examined.

Vibrational Sum-Frequency Spectroscopy

Vibrational sum-frequency spectroscopy (VSFS) is a surface-specific, nonlinear optical technique whose response is generated by coupling two coherent, high-intensity laser light sources spatially and temporally at an interface. [23−25] Only molecules that experience a noncentrosymmetric environment, such as those which feel the effects of an interface, can generate a VSFS response. The intensity of this response is governed by the square of the second-order polarizability $P^{(2)}$ through following expression

$$I_{SF} \propto |P^{(2)}|^2 \propto |\chi_{NR}^{(2)} e^{i\phi_{NR}} + \sum_{\nu} \chi_{R\nu}^{(2)} e^{i\gamma_\nu}|^2 I_{vis} I_{IR} \qquad (1)$$

where $P^{(2)}$ is the second-order polarization of the medium, $\chi_{NR}^{(2)}$ and $\chi_{R_\nu}^{(2)}$ are the nonresonant and resonant responses of the surface nonlinear susceptibility, $e^{i\phi_{NR}}$ and $e^{i\gamma_\nu}$ are the phases associated with those responses, and I_{vis} and I_{IR} are the intensities of the incident laser beams. The resonant contribution to the nonlinear susceptibility ($\chi_{R_\nu}^{(2)}$) can then be expressed as the following

$$(\chi_{R_\nu}^{(2)})_{IJK} \propto N \frac{A_K M_{IJ}}{\omega_\nu - \omega_{IR} - i\Gamma_\nu} \qquad (2)$$

where N is the number of responding molecules, A_K and M_{IJ} are the IR and Raman transition moments, respectively, ω_ν is the frequency of the vibrational resonance, ω_{IR} is the frequency of the incident IR beam, and Γ_ν is the natural line width of the transition. A vibrational mode must possess both nonzero IR and Raman transition moments to be sum-frequency active; such is the case for modes that lack inversion symmetry. Modes that possess local inversion symmetry, such as that found for methylene (CH_2) groups in an all-trans configuration along a surfactant backbone, will be sum-frequency inactive as a result of the local inversion symmetry canceling the sum-frequency response. For active modes, the intensity of the VSFS response is resonantly enhanced by tuning the IR frequency through a vibrational resonance, thus mapping out a spectrum of the interfacial molecules.

Spectral deconvolution and analysis of the VSFS data is based on a routine developed in our laboratory and modeled after the procedure first introduced by Bain et al.[26] Spectral fits are based on the expression

$$\chi_\nu^{(2)} = \int_{-\infty}^{\infty} \frac{A_\nu e^{-[\omega_L - \omega\nu/\Gamma\nu]^2}}{\omega_\nu - \omega_L - i\Gamma_L} d\omega_L \qquad (3)$$

which convolves the homogeneous line width of the transition (Γ_L) with an expression to account for inhomogeneous broadening (Γ_ν) due to the multitude of environments that the molecules experience in the condensed phase. A_ν represents the effective sum-frequency transition strength, which is proportional to the orientationally averaged IR and Raman transition moments, and ω_L and ω_ν are the center frequencies of the Lorentzian and Gaussian bands, respectively. We make use of a series of tightly held constraints on the peak phases, widths, and locations, obtained from spectra recorded in different environments, to attain curve fit parameters that are consistent across different interfacial systems. The phase of the individual peaks are allowed to fit from −3.14 to 3.14 rad about an arbitrarily assigned zero point (typically the CH_3(ss)). Fits resulting from a different zero point and/or constrained to be positive yielded the same relative phase information among the individual peak responses.

Experimental Section

Experiments were conducted using a diode-pumped Nd:YAG laser (Coherent, Infinity-100) that produces 3.5 ns pulses of 1064 nm light at a repetition rate of 20 Hz. The output of this laser was used to generate a fixed-frequency visible beam (532 nm) and a tunable IR beam (2700−3800 cm^{-1}), as has been described previously.[27] The energies of the input light at the sample were approximately 2.5 mJ for the 532 nm beam and 1−2 mJ (depending on wavelength) for the IR beam. Complete details of the laser system[27] and experimental setup[19,21] may be found elsewhere. All data were normalized to fluctuations of the IR power by measuring a portion of the IR beam split from the input IR beam with an identical path length. Spectra were obtained using SSP (s polarized sum frequency, s polarized visible, p polarized IR) polarization conditions.

Chemicals were used without further purification and include sodium oleate (Sigma-Aldrich, 99% pure), sodium stearate (Sigma-Aldrich, >99% pure), sodium decanoate (Sigma-Aldrich, 99−100% pure), sodium hexanoate (Sigma-Aldrich, 99−100% pure), sodium dodecyl sulfate (SDS, SigmaUltra, >99% pure), and D_2O (Cambridge Isotope Laboratories, 99.9%). All solutions were prepared at pH 5.1 using 18 MΩ water from a Nanopure filtration system. After each adsorption experiment, the cell and CaF_2 prism face were rinsed with copious amounts of Nanopure H_2O followed by vigorous stirring in 0.1 M HCl for 1 h. For the oleate experiments, an additional rinse in HPLC methanol for 1 h was necessary to remove the adsorbed oleate from the prism face; this was followed by another 0.1 M HCl rinse and H_2O rinse. Cleanliness of the prism and cell were checked by recording a Nanopure H_2O/CaF_2 spectrum prior to each experiment. The CaF_2 prism was cleaned more extensively between each different surfactant studied, as described previously.[21]

Equilibration of the system, following any additions made to the aqueous phase, was monitored by recording the signal intensity at the peak frequency of the water or CH_3 response over time (with stirring). Equilibration was considered complete when the sum-frequency intensity was constant (within noise) for 30 min. Five full spectra were recorded and averaged for each different solution composition. This procedure required taking spectra over a relatively long time period, thus ensuring that steady state was achieved for each solution condition.

Results

Oleate Adsorption to the CaF_2/Aqueous Interface. Sodium oleate is a common surfactant used for the separation of calcium-containing solid phases via the mineral flotation process.[18,28−30] The molecule consists of a negatively charged carboxylate headgroup and an 18-carbon alkyl backbone containing an olefinic cis double bond at the C_9 position (Figure 1). The adsorption of the oleate ion to the hydrophilic CaF_2/aqueous interface renders the surface of the solid phase hydrophobic,

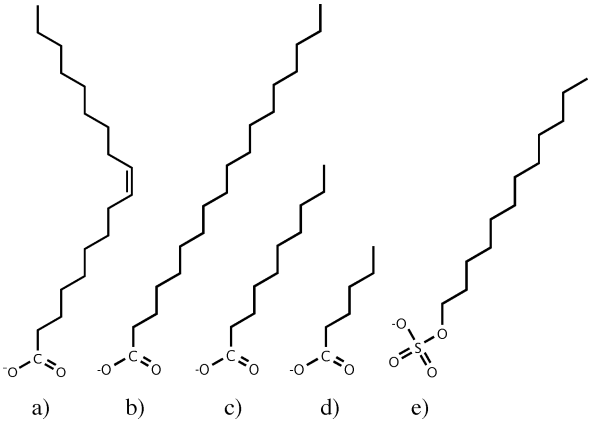

Figure 1. Surfactant molecules examined: (a) oleate, (b) stearate, (c) decanoate, (d) hexanoate, and (e) dodecyl sulfate.

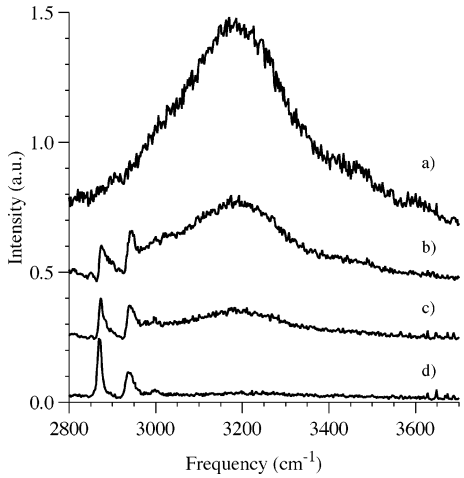

Figure 2. VSFS spectra of the CaF_2/H_2O/oleate interface at (a) neat CaF_2/H_2O and (b) 0.2, (c) 0.3, and (d) 0.4 μM oleate. Spectra are offset for clarity.

therefore allowing for the efficient separation of this phase from other minerals in solution.

Figure 2 shows the VSFS spectra in the OH stretching region, monitoring the adsorption of the negatively charged oleate ion to the CaF_2 surface. Figure 2a shows the spectrum of the neat CaF_2/H_2O interface at pH 5.1. There is a strong, broad response from highly coordinated interfacial water molecules centered around 3200 cm^{-1}, indicating strong orientation and ordering of water molecules near the CaF_2 surface. As has been described in previous studies,[19] the surface of CaF_2 takes on a positive charge when immersed in an aqueous phase as a result of the preferential dissolution of the surface fluoride ions. The positively charged surface aligns the interfacial water molecules and facilitates the formation of a collective water molecule network with a strong contribution at ~3200 cm^{-1} from these highly coordinated water molecules and a minor contribution at ~3450 cm^{-1} from more asymmetrically bound water molecules as shown in Figure 2a.

The addition of very low concentrations of oleate to the CaF_2/H_2O system (to a total oleate concentration of 0.2 μM) results in the spectrum shown in Figure 2b. The VSFS response from the interfacial water molecules has decreased considerably across the entire OH stretching region. The spectrum shows additional contributions in the 2800−3000 cm^{-1} region from the CH modes comprising the surfactant tail. Assignments for these modes will be discussed in detail in the D_2O studies presented later. The adsorption of the negatively charged oleate ion onto the positively charged CaF_2 surface steadily decreases the charge

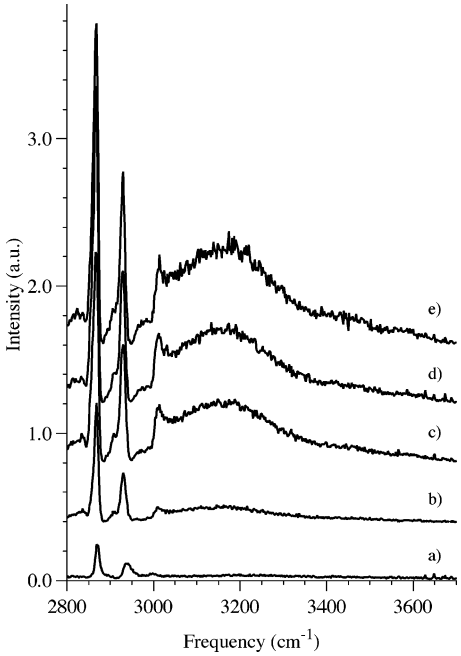

Figure 3. VSFS spectra of the CaF_2/H_2O/oleate interface at (a) 0.4, (b) 0.6, (c) 1.0, (d) 5.0, and (e) 50.0 μM oleate. Spectra are offset for clarity.

at that surface, resulting in a more random orientation of the interfacial water molecules. As the interfacial water molecules become more isotropic and therefore less sum-frequency active, there is a commensurate decrease in the signal from these molecules. Increasing the surfactant ion concentration from 0.2 to 0.3 and 0.4 μM results in the spectra shown in Figures 2c and 2d, respectively. The signal from the oriented interfacial water molecules has decreased as a function of increasing oleate ion concentration, until at 0.4 μM the signal from those interfacial H_2O molecules is essentially zero. There is also a steady increase in signal from the CH oscillators from the terminal methyl groups of the surfactant tails. The behavior of this system is consistent with an increase in the adsorption density of the negatively charged oleate ions onto the surface of the CaF_2, which decreases the electric field in the interfacial region and allows for complete randomization of the interfacial water molecules at ~0.4 μM.

Figure 3 shows the spectra of the CaF_2/H_2O/oleate interface at higher surfactant concentrations. Continued adsorption of the negatively charged oleate ions onto the surface of the CaF_2 solid now results in a steady *increase* in the signal from the OH stretching modes of the interfacial water molecules. In addition, there is a marked increase in the response from the terminal CH_3 groups of the adsorbed surfactant molecules. This trend continues until ~5 μM (Figure 3d), where the adsorption is essentially complete. A further 10-fold increase in concentration to 50 μM yields only minor changes in the overall intensity across the entire spectral region (Figure 3e).

The spectra presented in Figures 2 and 3 indicate that there is a steady adsorption of oleate ions onto the surface of the CaF_2 as the bulk concentration increases. On the basis of similar results from other surfactants at this interface,[20,21] we conclude that the drop and subsequent increase in the water OH mode intensities as a function of surfactant concentration is due to the alteration of the electric field present at the solid/liquid interface. The initially positively charged CaF_2 surface is neutralized during the adsorption of the anionic oleate ion (Figures 2a−d) with a subsequent decrease in the OH water band intensity. At higher surfactant ion concentrations, beyond

the point of surface charge neutralization, charge reversal and water reorientation occur as the negatively charged surfactant builds up on the surface (Figures 3a−e). As the electric field generated in the interfacial region increases, there is an increase in the number of water molecules aligned with that field, resulting in a larger signal from their OH modes.[31]

The strong response from the CH_3 modes in the spectra at higher concentrations indicates that the ordering of the surfactant tails increases with adsorption, facilitated by increased van der Waals interactions between the surfactant chains. The relatively densely packed monolayer formed on the surface of the CaF_2 orients the CH tails toward the aqueous phase, presenting a hydrophobic surface to the interfacial water molecules. The spectra shown in Figure 3 give no indication of water molecules directly above that hydrophobic monolayer that experience uncoupling of their OH modes due the differing bonding environments (aqueous vs hydrophobic) that the two OH bonds experience. These types of uncoupled OH modes have been detected in studies of other hydrophobic/aqueous interfaces.[27,32−35] In the studies presented here, either the surfactant layer formed in the CaF_2/H_2O/oleate system is not of sufficient density or regularity to give rise to this type of preferred orientation for the interfacial water molecules or the number of these uncoupled OH species is not sufficient enough to give rise to a detectable sum-frequency response.

To study, in more detail, the molecular conformation of the oleate ion in the absence of the spectral interferences from the OH modes of the interfacial water molecules, a series of experiments examining various surfactant concentrations were conducted in D_2O. Figure 4 shows the results of these adsorption experiments. Figure 4a shows the neat CaF_2/D_2O interface, which produces a featureless, low-intensity, nonresonant background across the spectral region from 2800 to 3100 cm^{-1}. Increasing the concentration of oleate ion from 0 to 0.3 μM results in the spectra shown in Figure 4b. The spectra show two very minor peaks at 2869 and 2932 cm^{-1}, which we assign to the symmetric stretching mode (r^+) of the terminal CH_3 groups along with its Fermi resonance (r^+-FR) from the adsorbed oleate molecules.[35−39] Recall that in the CaF_2/H_2O system there was a significant disruption of the interfacial water structure at this concentration resulting in a large decrease in signal from the more randomly oriented water molecules, as shown in Figure 2c. The fact that the CaF_2/D_2O system at this concentration shows only a minor response from these CH_3 groups indicates that the surfactant molecules have adsorbed in a relatively disordered fashion at this concentration. Further increases in oleate concentration to 0.4 and 0.5 μM result in a monotonic increase in the amplitude of the r^+ mode and its Fermi resonance from the terminal CH_3 groups, as shown in Figures 4c and 4d, respectively. The system passed through the point of zero charge (PZC) at ~0.4 μM (as indicated in the CaF_2/H_2O system, Figure 2d), yet the response from the CH modes of the adsorbed molecules is still relatively low, indicating a high degree of disorder of these molecules. Increasing the bulk oleate concentration to 0.8 μM results in a dramatic increase in the r^+ and r^+-FR modes as shown in Figure 4e. This corresponds with a similar increase in CH_3 intensity in the CaF_2/H_2O system at a similar concentration (Figure 3c). Also present in this spectra, to a very minor degree, are responses at 2846, 2952, and 3005 cm^{-1}, from the symmetric stretch (d^+) of the methylene CH_2 modes along the surfactant backbone, the antisymmetric (r^-) mode of the terminal CH_3 groups, and the CH stretching mode arising from the olefinic functional group at the C_9 position, respectively.[35−40] A plot

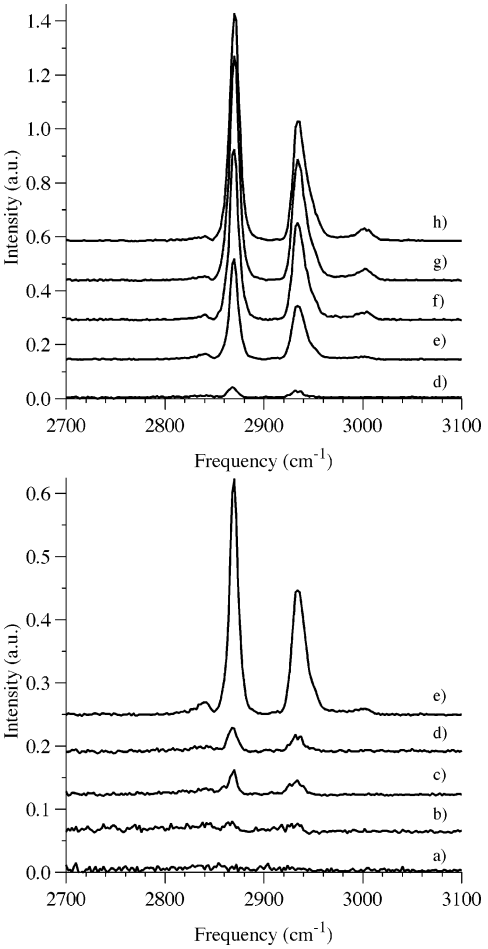

Figure 4. VSFS spectra of the CaF_2/D_2O/oleate interface at (a) neat CaF_2/D_2O and (b) 0.3, (c) 0.4, (d) 0.5, (e) 0.8, (f) 1.0, (g) 2.5, and (h) 5.0 μM oleate. Spectra are offset for clarity.

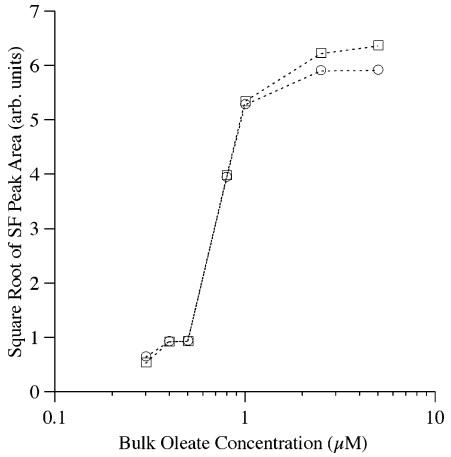

Figure 5. Plot of the integrated CH_3 (○) and CH_3-FR (□) peaks vs bulk oleate concentration for the CaF_2/D_2O/oleate system. Dashed lines are included as visual guides.

showing the dramatic rise in the integrated peak areas of the symmetric CH_3 (r^+) and CH_3 (r^+-FR) modes as a function of bulk oleate concentration is shown in Figure 5. The large, nonlinear increase in intensity of the CH modes over a relatively small concentration range is indicative of a higher degree of cooperative interaction among the oleate molecules on the surface of the CaF_2 than found at the lower surfactant concentrations. One explanation for this behavior is the onset of surfactant aggregates on the solid phase as a result of van der Waals attractions among the long carbon chains of the

adsorbed surfactant molecules.[16,41] At low surfactant concentrations, the molecules adsorb in a loosely packed fashion through electrostatic attraction to the oppositely charged solid surface. As the concentration of surfactant molecules in the interfacial region increases and reaches a critical value, the attractive van der Waals forces from the long-chain surfactant tails will begin to be a significant driving force for aggregation of these molecules. Adsorption at this critical concentration increases dramatically, and the molecules begin to form a more tightly packed monolayer via their self-assembly. The surfactant concentration where such strong aggregation occurs on a solid phase is often referred to as the critical hemimicelle concentration (CHMC). The surface CHMC is analogous to the solution critical micelle concentration (CMC) but is typically found at considerably lower concentrations.[42,43] This is especially true for systems where a large electrostatic surface component plays a significant role in increasing the local concentration of surfactant molecules in the interfacial region,[42] essentially raising the local surface concentration above the solution CMC. Our results indicate that the adsorption and aggregation of the oleate ions lead to the formation of a relatively densely packed, ordered monolayer on the surface of the CaF_2. Evidence for this conclusion comes from the dominating response from the terminal CH_3 and lack of significant response from either the CH_2 groups along the surfactant backbone or the antisymmetric (r^-) stretch of the terminal CH_3 mode at 2955 cm^{-1}. These results suggest that the oleate molecules are oriented with the symmetry axis of the terminal methyl groups nearly perpendicular to the interfacial plane and the majority of the CH_2 modes along the backbone of the surfactant in an all-trans configuration. Spectra recorded in SPS polarization (sum frequency, visible, IR) (not presented here) show response from only the antisymmetric (r^-) CH_3 stretch at 2955 cm^{-1}, confirming this orientation. This type of molecular configuration allows for significant van der Waals interactions between the surfactant molecules and therefore leads to the large increase in adsorption above 0.5 μM (which we take as the approximate value of the CHMC for this system).

At concentrations higher than the CHMC, the continued adsorption of surfactant molecules into the interfacial region is greatly diminished due to the increasing electrostatic repulsion of the more densely packed headgroups. Figures 4d−h present the spectra of the CaF_2/D_2O/oleate interface at oleate concentrations ranging from 0.8 to 5.0 μM. At oleate concentrations above 0.8 μM, there is still a slow but steady increase in the response from the pendant CH_3 groups, indicating that the adsorption and ordering of the oleate molecules are continuing but to a much lower degree (Figure 5). At 5.0 μM, the adsorption is essentially complete, with very little increase in intensity of the CH modes. These results parallel those from the CaF_2/H_2O/oleate system presented in Figure 3, where the increase in response from both the OH and CH modes reaches their largest values at this same concentration (5.0 μM).

To obtain further information about the orientation of molecules at the interface, we compare the results from the D_2O and H_2O studies, as presented in Figure 6. Figure 6a presents a selected D_2O spectrum showing all of the modes discussed above, without the interferences due to the OH oscillators. Figures 6b and 6c present spectra from the CaF_2/H_2O/oleate system at concentrations prior to and beyond the point of zero charge (PZC), respectively. In the two CaF_2/H_2O/oleate spectra (Figures 6b and 6c), there are clear changes in the interferences between the OH vibrational modes of the interfacial water molecules and the CH modes of the adsorbed surfactant. This

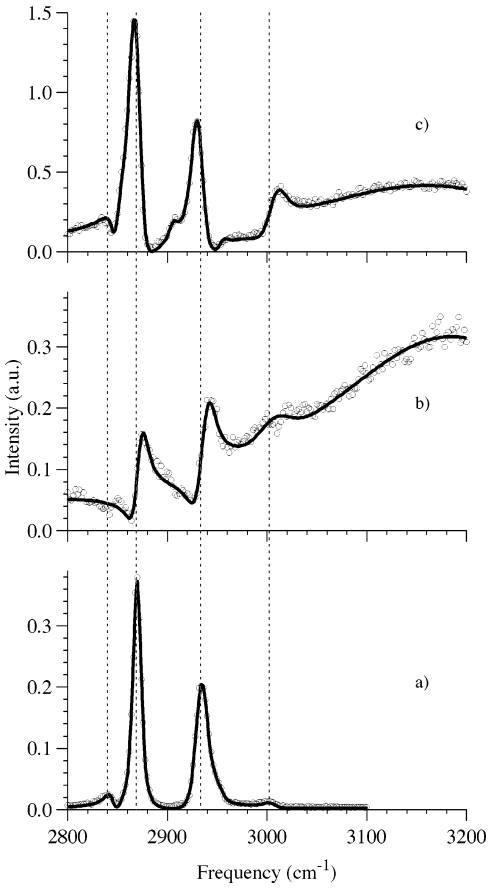

Figure 6. VSFS spectra (symbols) and curve fits (solid line) for (a) the 0.8 μM CaF_2/D_2O/oleate interface, (b) the 0.2 μM CaF_2/H_2O/oleate interface, and (c) the 0.6 μM CaF_2/H_2O/oleate interface.

is especially evident in comparing the asymmetries on either side of the peak maximums at 2869 and 2932 cm^{-1} (determined from the D_2O studies) for the two H_2O systems. The interferences give rise to apparent peak shifts from the unperturbed D_2O values and show changes to the overall shape of the transition on either side of the peak center. As was shown in our previous studies on the CaF_2/H_2O/SDS system,[21] we use these interferences to attain relative orientation information about molecules in the interfacial region. We fit the three data sets using tightly constrained fitting parameters for the CH modes and two additional responses for the OH modes of the interfacial water molecules. The phase of these OH modes is held fixed at either 180° or 0° for the positively or negatively charged interface, respectively. At concentrations prior to the PZC (Figure 6b), when the CaF_2 surface is positively charged, the interfacial water molecules orient with their oxygen atoms pointing toward the surface of the solid phase, resulting in a destructive interference between spectral response of the OH modes with the CH modes from the adsorbed surfactant molecules. At higher bulk surfactant concentrations (Figure 6c), the surface charge reverses and reorients the interfacial water molecules with their hydrogen atoms pointing toward the now negatively charged surfactant/solid surface. The 180° reorientation results in a 180° phase change between the OH and CH modes, evident in the overall change in shape in the 2850−3100 cm^{-1} region (and especially near the transitions at 2869 and 2932 cm^{-1}) in Figures 6b and 6c. As is evident in the results shown in Figure 6, we can achieve a very good fits across all three data sets, which is consistent with the charge reversal and reorientation of the interfacial water molecules near the solid

TABLE 1: Parameters Determined from the Nonlinear Least-Squares Fits to the Experimental Data[a]

oscillator	amplitude (arb. units)	frequency (cm^{-1})	width (Γ_L) (cm^{-1})	width (Γ_v) (cm^{-1})	phase (rad)
CaF_2/H_2O/Oleate System at 0.2 μM Oleate, Prior to Charge Reversal					
CH_3 (ss)	0.53	2869	2	6	0.0
CH_3 (ss-FR)	0.37	2932	2	8	0.0
H_2O (ss)	0.37	3217	5	149	3.14
H_2O (ss)	0.11	3463	5	99	3.14
CaF_2/H_2O/Oleate System at 0.6 μM Oleate, Past Charge Reversal					
CH_2 (ss)	0.33	2848	2	4	−1.6
CH_3 (ss)	1.55	2870	2	6	0.0
CH_3 (ss-FR)	1.01	2932	2	6	0.0
=CH (ss)	0.33	3005	2	7	2.2
H_2O (ss)	0.65	3178	5	174	0.0
H_2O (ss)	0.15	3457	5	110	0.0
CaF_2/D_2O/Oleate System at 0.8 μM Oleate					
CH_2 (ss)	0.16	2846	2	5	−1.0
CH_3 (ss)	0.95	2870	2	4	0.0
CH_3 (ss-FR)	0.55	2934	2	7	0.0
=CH (ss)	0.18	3009	2	7	2.5

[a] Spectra are presented in Figure 6.

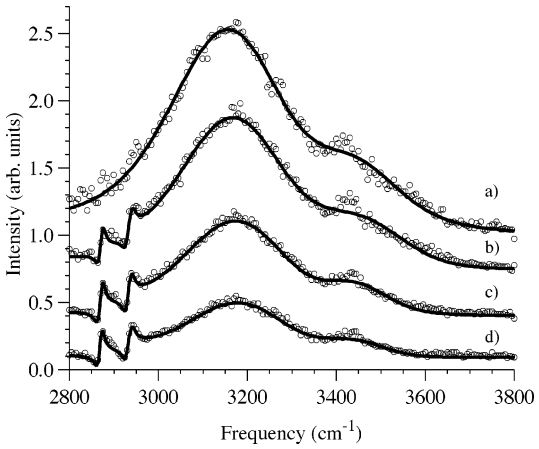

Figure 7. VSFS spectra (symbols) and curve fits (solid line) of the CaF_2/H_2O/stearate interface at (a) neat CaF_2/H_2O and (b) 5.6, (c) 11.0, and (d) 18.0 μM stearate. Spectra are offset for clarity.

surface due to the adsorption of the oleate molecules. The fitting parameters for all of these spectra are included in Table 1.

Stearate Adsorption to the CaF_2/H_2O Interface. The stearate ion is nearly identical to the oleate ion presented in the above sections; however it is lacking the olefinic double bond at the C_9 position (Figure 1). The sodium salt of the stearate ion has a considerably lower solubility in water, which manifests itself in a much lower surface activity compared to oleate. The adsorption behavior of stearate at the CaF_2 interface mirrors that of the CaF_2/H_2O/oleate experiments; however the concentrations necessary for a similar reduction in OH response upon initial adsorption are 1−2 orders of magnitude higher than found in the oleate system. Figure 7 shows the CaF_2/H_2O/stearate interface as a function of bulk stearate concentration, beginning with the neat CaF_2/H_2O interface shown in Figure 7a. Addition of stearate ion to a concentration of 5.6 μM is presented in Figure 7b. The response from the interfacial water molecules has decreased by ∼20% (by peak area) at both 3200 and 3430 cm^{-1}. There are relatively strong responses from the CH_3 groups present on the adsorbed surfactant that show up as destructive interferences with the OH modes in the 2800−3000 cm^{-1} region. Figures 7c and 7d show further increases in bulk surfactant concentration to 11 and 18 μM, respectively. These concentration increases result in a continuation of the general trend of decreasing signal from interfacial water molecules and an increasing signal from the CH_3 groups from the adsorbed surfactant. Peak-fitting analysis of these spectra indicate that there is a steady decrease in the OH signal of ∼65% from the neat CaF_2/H_2O interface to the 18 μM system, with a commensurate increase in signal from the CH_3 modes of ∼100% between the 5.6 and 18 μM systems. Thus, similar to the CaF_2/H_2O/oleate system, stearate molecules steadily adsorb and associate on the CaF_2 surface, resulting in a decrease in the interfacial potential followed by randomization of water molecules near that surface. This randomization leads to the steady decrease in the signal from the OH oscillators of these interfacial species.

A small increase in bulk stearate concentration from 18 to 19 μM results in an unusually large increase in the degree of adsorption in this system. After the concentration increase, the signal from the interfacial water molecules decreases steadily, passes through a minimum, and begins steadily increasing again as the stearate molecules adsorb into the interfacial region. Figure 8 shows the spectrum recorded for the 19 μM CaF_2/H_2O/stearate system. There is a substantial increase in the signal from CH_3 groups at 2872 and 2932 cm^{-1} as well as a relatively large signal response from the OH stretch of the interfacial water molecules at 3200 and 3430 cm^{-1}. We attribute both of these changes to a sharp increase in stearate adsorption at this concentration. The time to reach a steady-state condition after this concentration increase was found to be significantly longer than that for earlier increases. The time dependence of this system will be explored in detail in the next section. The change in the interferences between the CH and OH modes shown in Figure 8 as compared to those shown in Figure 7 indicates that the water molecules near the solid surface have reoriented by 180°, similar to the oleate system. This reorientation was confirmed in the curve fits shown in Figure 8, which include a 180° change in phase for the OH oscillator responses at 3200 and 3430 cm^{-1}. This spectrum also includes a minor peak at 3674 cm^{-1} that we assign to the OH stretch of uncoupled, weakly bound water molecules straddling the interface between the aqueous phase and the hydrophobic self-assembled monolayer of stearate molecules on the CaF_2 surface (see depiction in Figure 8). These weakly interacting water molecules with one OH bond penetrating into a hydrophobic interface and the other participating in hydrogen bonding with water molecules in the aqueous phase have been observed in a variety of systems ranging from neat air/H_2O,[32,44,45] CCl_4/H_2O,[27,34] and alkane/H_2O[46] to water molecules interacting with hydrophobic octadecyltrichlorosilane (OTS) monolayers self-assembled onto silica substrates.[35] However, this is the first time that these species have been reported for a semisoluble salt/H_2O interface whose surface is presumably rather rough.

The spectrum of the CaF_2/H_2O/stearate system at 19 μM indicates that the adsorbed surfactant molecules have formed a highly ordered, densely packed monolayer on the surface of the CaF_2 solid. This is evident in the very large response from the CH_3 oscillators and the lack of response from CH_2 oscillators along the stearate backbone (the local inversion symmetry of the CH_2 modes in an all-trans configuration renders these modes sum-frequency inactive). Gauche defects in the adsorbed chains would give rise to a peak in the 2840−2850 cm^{-1} region. These two aspects, taken together, show that the stearate molecules have self-assembled into a highly ordered layer on the solid surface. Although we did not conduct bulk isotherm experiments for this system and therefore cannot be certain a "complete" monolayer is formed on the CaF_2 surface, stearate adsorption

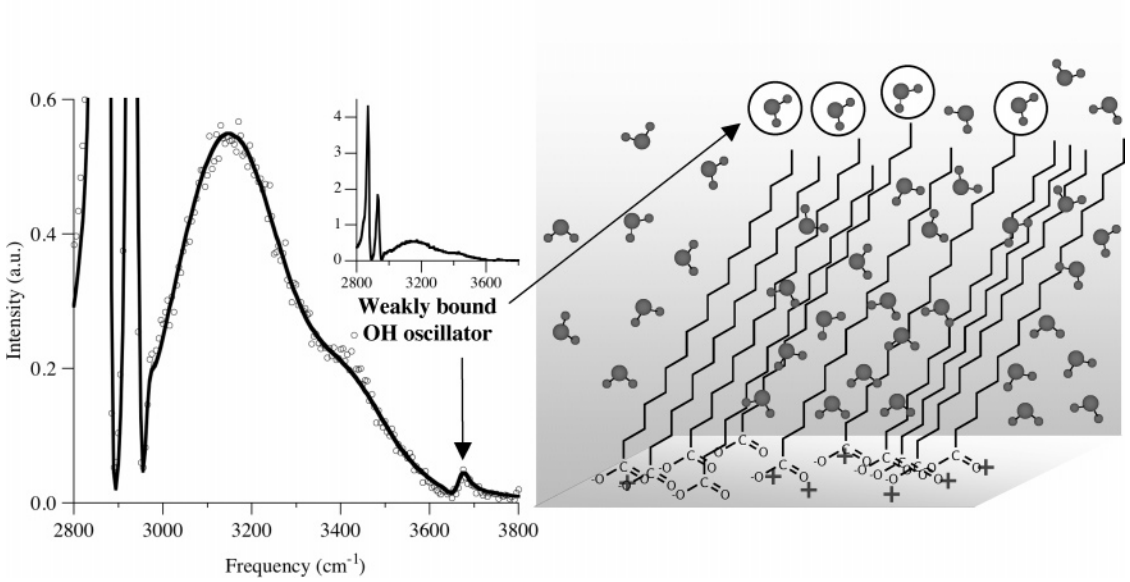

Figure 8. VSFS spectra (symbols), curve fits (solid line), and cartoon representation of the CaF_2/H_2O/stearate interface at 19 μM.

appears to reach a plateau at this concentration (19 μM), with further increases in concentration (up to 40 μM) showing no further changes in the VSFS response from either the OH or the CH modes. In addition, the presence of weakly bound OH oscillators at 3674 cm^{-1} indicates that the self-assembled monolayer forms a relatively sharp interface with water, giving rise to a small number of uncoupled water molecules. This free-OH mode is similar in frequency to those found at other hydrophobic/aqueous interfaces such as H_2O/hexane (3674 cm^{-1})[46] and octadecyltrichlorosilane (OTS) monolayers on SiO_2 (3674 cm^{-1}).[35] In contrast, spectra from both the CaF_2/H_2O/oleate system and the CaF_2/H_2O/SDS system[21] show considerably lower response from the CH_3 oscillators and the presence of at least minor gauche defects (quite significant in the CaF_2/H_2O/SDS system[21]) and lack any response from the weakly bound OH oscillators in the 3600−3700 cm^{-1} region, indicating that these systems form less distinct monolayers that are considerably more disordered and/or less dense than those generated in the CaF_2/H_2O/stearate system. These results show that although there is the potential for significant van der Waals interactions among the long-chain oleate molecules the presence of the more rigid double bond in the middle of the surfactant backbone restricts the ability for these molecules to pack as tightly as those monolayers found in the stearate studies or to form a relatively sharp interface. This more open structure allows water molecules to penetrate the adsorbed chains and further disrupt the oleate monolayer. Experiments comparing the contact angle of water droplets on stearate and oleate monolayers formed on the surface of solid CaF_2 indicate that the oleate monolayers have lower contact angles and higher surface area per molecule than those found in the CaF_2/H_2O/stearate systems.[47] The contact angles for the CaF_2/H_2O/stearate system are closer to those found in highly ordered, densely packed, hydrophobic OTS monolayers formed on the surface of SiO_2,[47] indicating that stearate molecules also form this type of strongly hydrophobic surface.

Previous adsorption studies examining the CaF_2/H_2O/SDS and CaF_2/D_2O/SDS interfaces reveal that sodium dodecyl sulfate adsorption onto the CaF_2 surface results in the formation of highly disordered monolayers followed by bilayer formation at high surfactant concentration.[21] In contrast to these SDS studies, both the oleate and the stearate systems described in the previous sections show no indication for the formation of surfactant bilayers. Both systems show a steady, monotonic increase in response from the CH_3 modes across a large concentration range (Figures 4 and 9). Studies on the CaF_2/D_2O/SDS system reveal that there is a steady decrease in the response from the CH_3

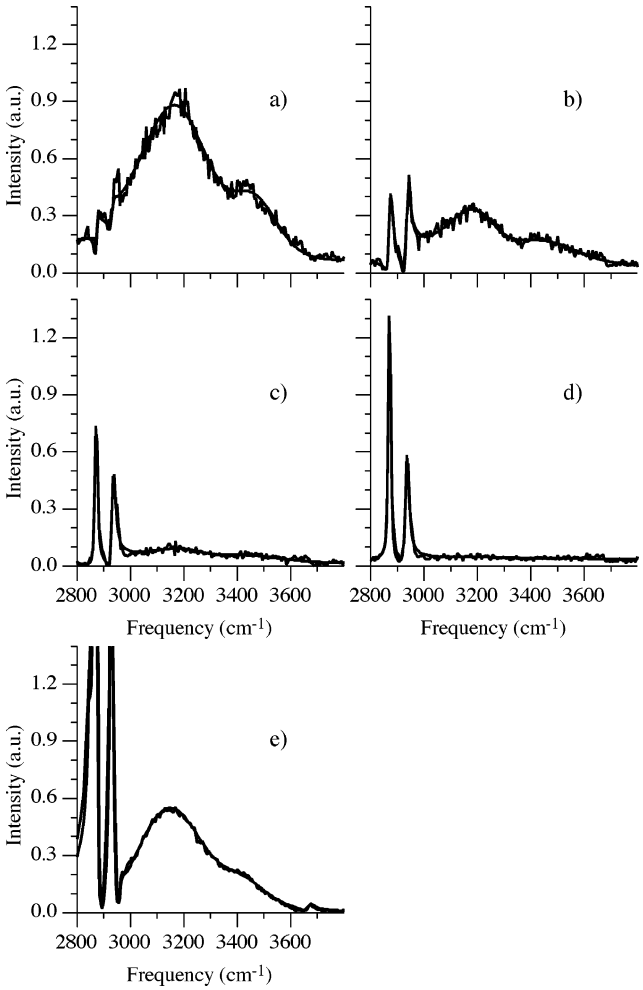

Figure 9. VSFS spectra recorded as a function of time for the CaF_2/H_2O/stearate interface following a stearate concentration increase from 12 to 19 μM. Part a was recorded immediately after the concentration increase followed by (b) 2, (c) 3, (d) 4, and (e) 24 h. Gray lines are actual data; black lines are curve fits to the data.

oscillators as the bulk surfactant concentration is increased due to the more centrosymmetric environment arising from the formation of the surfactant bilayer. In addition, at relatively high bulk surfactant concentrations (on the order of 10−100 times those found in the stearate and oleate studies), spectra recorded for SDS adsorption beyond the point of surface charge neutralization include a new feature at 3580 cm^{-1}, assigned to the solvation of the sulfate headgroups oriented toward the aqueous phase in a bilayer structure.[20] The fact that in the oleate and stearate systems the signal from the terminal CH_3 modes steadily increases as a function of surfactant concentration indicates that adsorption of the surfactant ions into the interfacial region is characterized by continued monolayer formation rather than bilayer formation. If bilayer formation was initiated in these systems, then the response from these terminal methyl groups should decrease or remain the same as the surfactant concentration is increased. In addition, both the stearate and the oleate systems show no indication of a solvation peak at surfactant concentrations beyond the point of charge neutralization, as is found in the CaF_2/H_2O/SDS system. Both of the carboxylate surfactant systems appear to reach a plateau in adsorption with only minor changes to the intensity and overall shape of the spectra with further increases in concentration.

Dynamics of Stearate Adsorption at the CaF_2/H_2O Interface. As presented in the last section, a small increase in bulk stearate concentration from 18 to 19 μM results in a significant increase in the level of adsorption in this system. In addition, the time to reach a steady-state condition was found to be significantly longer than that found for the earlier concentration increases (on the order of 4−5 h, compared to 30 min for the earlier additions). Taking advantage of this slow equilibrium, we are able to monitor the adsorption process in the CaF_2/H_2O/stearate system by recording spectra across the entire 2800−3800 cm^{-1} region as a function of time. Figure 9 presents a series of spectra taken over a 24 h period, following the addition of stearate ion from 12 to 19 μM. Figure 9a shows the spectrum of an equilibrated solution of 12 μM stearate ion adsorbed to the surface of the solid phase. The characteristic peaks from the ordered interfacial water molecules are quite strong at this concentration, and the CH interferences due to the adsorbed stearate molecules are also clearly evident. The concentration of stearate ion was then increased to 19 μM ($t = 0$ h). Figure 9b shows the spectrum of this system after a 2 h equilibration time. There has been a significant decrease in the OH stretching response and an increase in the CH response as a result of the adsorption of the surfactant onto the solid surface. Note that all of the spectra required approximately 10 min to record, a time frame we found to be acceptable to minimize alterations in the spectral response during the scan. Figures 9c and 9d show this same system after 3 and 4 h, respectively. Over this time period, the response from the interfacial water molecules steadily decreases to approximately zero while the response from the CH_3 modes steadily increases as a result of the continued adsorption of the stearate ions. The spectrum recorded at 4 h shows only signal from the CH_3 modes, with little interference from any OH mode contributions, very similar to that found in the oleate/D_2O spectra. The system was then allowed to equilibrate for 24 h, and the spectra shown in Figure 9e was recorded. As shown in this figure, the intensity of the CH_3 response has increased dramatically as has the signal from the interfacial water molecules at 3200 and 3430 cm^{-1} and the weakly bound, uncoupled OH oscillators at 3674 cm^{-1}. Spectra recorded at later times showed no change in signal level, indicating that a steady state had been achieved. Further increases in stearate concentration yielded only minor changes to the spectrum, also indicating that the adsorption was complete.

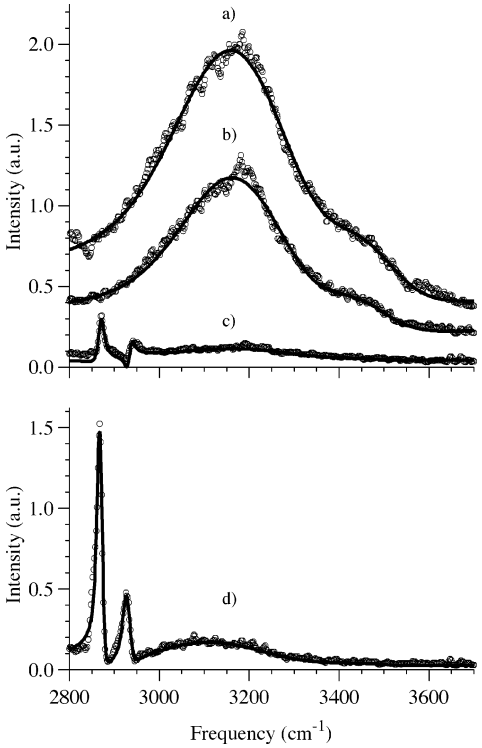

Figure 10. VSFS spectra (symbols) and curve fits (solid line) of the CaF_2/H_2O/decanoate interface at (a) neat CaF_2/H_2O and (b) 4, (c) 140, and (d) 190 μM decanoate. Spectra a and b are offset for clarity.

As Figure 9 shows, adsorption of stearate ions at 19 μM leads to the slow, steady formation of a densely packed monolayer on the surface of the CaF_2 over a 24 h equilibration time. The adsorption leads to an increase in the signal from the pendant CH_3 groups as the surfactant molecules adsorb and order on the solid surface. The steadily decreasing surface charge, as a result of the adsorption of stearate ions, leads to the randomization of the interfacial water molecules with a commensurate decrease in their VSFS signal (between $t = 0$ and $t = 4$ h). After a 24 h equilibration time, the surfactant ions form of a highly ordered, densely packed monolayer on the solid surface, resulting in a dramatic increase in CH_3(ss) signal, an increase in the structured water molecule signal, and the presence of weakly interacting, uncoupled OH modes responding at 3674 cm^{-1} from water molecules interacting with the hydrophobic surface generated on the solid surface.

Adsorption of Shorter-Chain Carboxylate Surfactants to the CaF_2/H_2O Interface. To further investigate the carboxylate surfactants, we conducted a series of experiments studying the effect of chain length on the overall adsorption behavior of these ions. Figures 10 and 11 present the spectra of shorter-chain carboxylate surfactants decanoate (C_{10}) and hexanoate (C_6) adsorbed at the CaF_2/H_2O interface, respectively. Both of these ions have considerably higher solubilities in water than either stearate or oleate. Figure 10a shows the CaF_2/H_2O interface. Upon an increase in the concentration to 4 μM decanoate, the OH signal from interfacial water molecules decreases only slightly, and there is no indication of any CH resonances. We note that at these concentrations in both the oleate and the stearate experiments there was a marked change in the spectra compared to the neat CaF_2/H_2O system (Figures 3d and 7b). Increasing the decanoate concentration to 140 μM results in the adsorption of the decanoate ion to the point of near charge neutralization as shown in Figure 10c. There is a small response

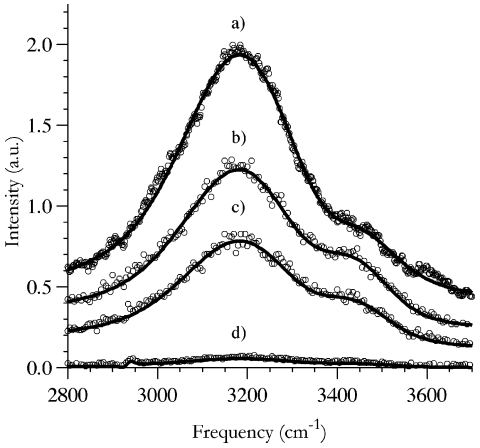

Figure 11. VSFS spectra (symbols) and curve fits (solid line) of the CaF_2/H_2O/hexanoate interface at (a) neat CaF_2/H_2O and (b) 5600, (c) 13 000, and (d) 40 000 μM hexanoate. Spectra are offset for clarity.

in the 3200 cm^{-1} region and minor responses from the adsorbed CH_3 modes. Increasing the concentration to 190 μM results in the spectrum shown in Figure 10d, where there is now a strong response from the CH_3 resonances and a small response from the interfacial water molecules. Again, as seen in the oleate and stearate systems, further increases to the surfactant ion concentration lead to only minor increases in these peaks, indicating that the adsorption is complete.

Figure 11 shows the adsorption behavior of the hexanoate ion to the CaF_2/H_2O interface. The adsorption behavior is similar to all of the above systems; however the concentration required to initiate the adsorption process and to achieve charge neutralization is considerably higher than for any other system studied. Figure 11d shows the spectra of the CaF_2/H_2O/hexanoate interface at a concentration of 40 000 μM hexanoate. The response from the interfacial water molecules is nearly zero, indicating that the system was very near surface charge neutralization. However, increases in surfactant ion concentration beyond this concentration did not show any indication of continued adsorption, and the signal levels from the CH and OH oscillators remained unchanged. There is no evidence in the 3650−3700 cm^{-1} region for uncoupled water molecules for either the hexanoate or the decanoate systems, indicating that these monolayer/water interfaces are relatively rough.

As the above spectra show, the adsorption of the shorter-chain C_{10} and C_6 surfactants requires considerably higher concentrations to achieve charge neutralization and plateau adsorption as compared to the longer-chain C_{18} surfactants. This indicates that the adsorption process is not only initiated by the electrostatic attraction between the positively charged CaF_2 surface and the negatively charged surfactant ion but is also highly dependent on the van der Waals interactions among the surfactant tails.

Conclusions

We have presented the results of our VSFS studies of a series of carboxylate surfactant ions adsorbing onto the surface of the semisoluble solid CaF_2. All of the carboxylate surfactants show formation of monolayers on the surface of the CaF_2 solid at adsorption saturation. In each case, surfactant adsorption and monolayer formation have a significant effect on the structure and orientation of interfacial water molecules during the adsorption process. The surface charge of the CaF_2 solid is steadily passivated as the concentration of the surfactant ions is increased. Each system reaches a point of surface charge neutralization at considerably different concentrations. Continued adsorption beyond the point of surface charge neutralization reverses the charge in the interfacial region, resulting in a 180° reorientation and reformation of the highly coordinated water molecule network in the interfacial region. The extent of adsorption was found to be highly dependent on the chain length of the surfactant ions, with the long-chain ions adsorbing at significantly lower concentrations than the shorter-chain ions possessing similar headgroups. Data comparing the concentration where charge neutralization was achieved is presented in Table 2. The adsorption behavior of these ions spans a concentration range of 5 orders of magnitude, depending on the chain length and headgroup of the ion examined. The longer-chain surfactants formed tightly packed, well-ordered monolayers as shown by significant response from the terminal CH_3 modes and lack of response from CH_2 modes along the surfactant backbone. The stearate system is distinguished by a large increase in adsorption over a very small concentration range, leading to formation of very tightly packed monolayers over long equilibration times. The presence of weakly bound, uncoupled OH oscillators at saturation coverage indicates that these self-assembled monolayers form a relatively abrupt hydrocarbon/water interface. The frequency of the weakly bound OH oscillators found at this interface is similar to that observed at other hydrophobic/aqueous interfaces. This is the first molecular-level confirmation of the formation of such well-ordered, hydrophobic monolayers on the surface of an ionic solid such as CaF_2. The shorter-chain surfactants formed more disordered monolayers at much higher concentrations due to the lack of significant van der Waals interactions between the shorter chains. There is no evidence for bilayer formation in any of the carboxylate surfactant/H_2O systems as has been observed in the CaF_2/H_2O/SDS system.

TABLE 2: Comparison of the Charge Neutralization Concentration for the Surfactants Studied

surfactant	concentration at PZC (μM)	headgroup	chain length
oleate	0.4		C_{18} (*cis*-C_9=C_{10})
stearate	18		C_{18}
decanoate	140		C_{10}
hexanoate	40 000		C_6
SDS[21]	200		C_{12}

Acknowledgment. We gratefully acknowledge the financial support of the Department of Energy, Basic Energy Sciences, DE-FG-02-96ER4557.

Note Added after ASAP Publication. This Article was published on Articles ASAP on March 2, 2005, without the Acknowledgment. The corrected Article was posted March 4, 2005.

References and Notes

(1) *Surfactant Adsorption and Surface Solubilization*; Sharma, R., Ed.; ACS Symposium Series 615; American Chemical Society: Washington, DC, 1995.

(2) Myers, D. *Surfaces, Interfaces, and Colloids. Principles and Applications*, 2nd ed.; John Wiley & Sons: New York, 1999.
(3) Adamson, A. W.; Gast, A. P. *Physical Chemistry of Surfaces*, 6th ed.; John Wiley & Sons: New York, 1997.
(4) Hanna, H. S.; Somasundaran, P. Flotation of Salt-Type Minerals. In *Flotation: A. M. Gaudin Memorial Volume*; Fuerstenau, M. C., Ed.; American Institute of Mining, Metallurgical, and Petroleum Engineers, Inc.: New York, 1976; Vol. 1, p 197.
(5) Free, M. L.; Miller, J. D. *Langmuir* **1997**, *13*, 4377.
(6) Wu, L.; Forsling, W. *J. Colloid Interface Sci.* **1995**, *174*, 178.
(7) Hancer, M.; Celik, M. S.; Miller, J. D. *J. Colloid Interface Sci.* **2001**, *235*, 150.
(8) Hu, Y.; Lu, Y.; Veeramasuneni, S.; Miller, J. D. *J. Colloid Interface Sci.* **1997**, *190*, 224.
(9) Holmgren, A.; Wu, L.; Forsling, W. *Spectrochim. Acta, Part A* **1994**, *50*, 1857.
(10) Barraclough, P. B.; Hall, P. G. *J. Chem. Soc., Faraday Trans.* **1975**, *71*, 2266.
(11) Kuroda, Y. *J. Chem. Soc., Faraday Trans.* **1985**, *81*, 757.
(12) Kuroda, Y.; Sato, H.; Morimoto, T. *J. Colloid Interface Sci.* **1985**, *108*, 341.
(13) Gonzalez-Martin, M. L.; Rochester, C. H. *J. Chem. Soc., Faraday Trans.* **1992**, *88*, 873.
(14) Popping, B.; Deratani, A.; Sebille, B.; Desbois, N.; Lamarche, J. M.; Foissy, A. *Colloids Surf.* **1992**, *64*, 125.
(15) Drelich, J.; Atia, A. A.; Yalamanchili, M. R.; Miller, J. D. *J. Colloid Interface Sci.* **1996**, *178*, 720.
(16) Drelich, J.; Jang, W.-H.; Miller, J. D. *Langmuir* **1997**, *13*, 1345.
(17) Mielczarski, E.; de Donato, P.; Mielczarski, J. A.; Cases, J. M.; Barres, O.; Bouquet, E. *J. Colloid Interface Sci.* **2000**, *226*, 269.
(18) Mielczarski, E.; Mielczarski, J. A.; Cases, J. M. *Langmuir* **1998**, *14*, 1739.
(19) Becraft, K. A.; Richmond, G. L. *Langmuir* **2001**, *17*, 7721.
(20) Becraft, K. A.; Moore, F. G.; Richmond, G. L. *J. Phys. Chem. B* **2003**, *107*, 3675.
(21) Becraft, K. A.; Moore, F. G.; Richmond, G. L. *Phys. Chem. Chem. Phys.* **2004**, *6*, 1880.
(22) Moore, F. G.; Becraft, K. A.; Richmond, G. L. *Appl. Spectrosc.* **2002**, *56*, 1575.
(23) Bloembergen, N.; Pershan, P. S. *Phys. Rev.* **1962**, *128*, 606.
(24) Zhu, X. D.; Suhr, H.; Shen, Y. R. *Phys. Rev. B* **1987**, *35*, 3047.
(25) Guyot-Sionnest, P.; Hunt, J. H.; Shen, Y. R. *Phys. Rev. Lett.* **1987**, *59*, 1597.
(26) Bain, C. D.; Davies, P. B.; Ong, T. H.; Ward, R. N. *Langmuir* **1991**, *7*, 1563.
(27) Scatena, L. F.; Richmond, G. L. *J. Phys. Chem. B* **2001**, *105*, 11240.
(28) Finkelstein, N. P. *Trans. Inst. Min. Metall., Sect. C* **1989**, *98*, C157.
(29) Mielczarski, J. A.; Mielczarski, E.; Cases, J. M. *Langmuir* **1999**, *15*, 500.
(30) Free, M. L.; Miller, J. D. *Int. J. Miner. Process.* **1996**, *48*, 197.
(31) Gragson, D. E.; Richmond, G. L. *J. Am. Chem. Soc.* **1998**, *120*, 366.
(32) Du, Q.; Freysz, E.; Shen, Y. R. *Science* **1994**, *264*, 826.
(33) Baldelli, S.; Schnitzer, C.; Shultz, M. J.; Campbell, D. J. *J. Phys. Chem. B* **1997**, *101*, 10435.
(34) Scatena, L. F.; Brown, M. G.; Richmond, G. L. *Science* **2001**, *292*, 908.
(35) Ye, S.; Nihonyanagi, S.; Uosaki, K. *Phys. Chem. Chem. Phys.* **2001**, *3*, 3463.
(36) Watry, M. R.; Richmond, G. L. *Langmuir* **2002**, *18*, 8881.
(37) Goates, S. R.; Schofield, D. A.; Bain, C. D. *Langmuir* **1999**, *15*, 1400.
(38) Liu, Y.; Wolf, L. K.; Messmer, M. C. *Langmuir* **2001**, *17*, 4329.
(39) Himmelhaus, M.; Eisert, F.; Buck, M.; Grunze, M. *J. Phys. Chem. B* **2000**, *104*, 576.
(40) Tandon, P.; Neubert, R.; Wartewig, S. *J. Mol. Struct.* **2000**, *526*, 49.
(41) Somasundaran, P.; Fuerstenau, D. W. *J. Phys. Chem.* **1966**, *70*, 90.
(42) Besio, G. J.; Prud'homme, R. K.; Benziger, J. B. *Langmuir* **1988**, *4*, 140.
(43) Fuerstenau, D. W. *J. Colloid Interface Sci.* **2002**, *256*, 79.
(44) Raymond, E. A.; Tarbuck, T. L.; Richmond, G. L. *J. Phys. Chem. B* **2002**, *106*, 2817.
(45) Raymond, E. A.; Tarbuck, T. L.; Brown, M. G.; Richmond, G. L. *J. Phys. Chem. B* **2003**, *107*, 546.
(46) Brown, M. G.; Walker, D. S.; Raymond, E. A.; Richmond, G. L. *J. Phys. Chem. B* **2003**, *107*, 237.
(47) Jang, W.-H.; Drelich, J.; Miller, J. D. *Langmuir* **1995**, *11*, 3491.